Theoretical description of the ejected-electron spectrum in collisions of 1.5-MeV/u F^{9+} with helium

D. R. Schultz
Physics Division, Oak Ridge National Laboratory, Oak Ridge, Tennessee 37831-6373

C. O. Reinhold
University of Tennessee, Knoxville, Tennessee 37996-1200
and Oak Ridge National Laboratory, Oak Ridge, Tennessee 37831-6377
(Received 9 March 1994)

We present the results of an extensive classical trajectory Monte Carlo simulation of the ejected electron spectrum in collisions of 1.5-MeV/u F^{9+} with helium. Excellent agreement is found with the measurements of Lee *et al.* [Phys. Rev. A **41**, 4816 (1990)] for ejection to 0°. In particular, the simulation reproduces extremely well the shape and magnitude of the electron-capture-to-the-continuum and binary peaks. We contrast this agreement with calculations utilizing various quantum-mechanical perturbation theories. Also, a continuum-distorted-wave–eikonal-initial-state approach, which describes the interaction between the outgoing electron and the residual target ion through a model potential, has been utilized. This approach is shown to be an improvement over conventional calculations based on the use of effective charges. We draw conclusions regarding the proper representation of the collision dynamics leading to electron ejection in the low-energy, electron-capture-to-the-continuum, and binary peak regimes. Calculations of the doubly differential ionization cross section for non-0° ejection are displayed as well.

PACS number(s): 34.50.Fa, 34.10.+x

I. INTRODUCTION

The study of the ejected-electron spectrum resulting from ion-atom collisions has lead to a fuller understanding of the processes involved in ionization and to strenuous tests of theoretical approaches [1, 2]. In particular, details have been elucidated concerning the formation and resulting degree of asymmetry of the electron-loss or -capture cusp, the magnitude, shape, and position of the binary peak, and the important role played by the saddle-point mechanism for ejection of low-energy electrons. Such investigation is of both fundamental and practical interest in that the study of ionization provides a basic testing ground for theoretical and experimental treatments, while also serving to provide information of relevance to technological development. For example, an accurate description of the energy and angle distribution of ejected electrons forms the basis for modeling the damage caused in ion-impact of semiconductors, caused intentionally to etch or otherwise process the material, or unintentionally as in cosmic ray bombardment of spaceborne electronics [3]. Also, since the greatest energy deposition in solids such as human tissue is caused by the very hottest electrons released in ion-atom collisions, those of the binary peak, understanding of this feature of the ejected-electron spectrum is of primary importance for modeling the radiological treatment of disease or biological damage caused by heavy particle radiation [4–6].

We present here theoretical results utilizing an extensive classical trajectory Monte Carlo (CTMC) simulation, an approach which makes use of the time evolution of a quasi-classical ensemble representing the wave function. These results are compared with the experimental measurements of the doubly differential ionization cross section obtained by Lee *et al.* [7] for 0° ejection in the laboratory and with other approaches based on quantal perturbation theory (first Born, continuum-distorted-wave, and distorted-wave strong potential Born approximations). A close examination is made of the spectrum of electrons ejected near the cusp and the binary peak to highlight the dynamic mechanisms and the differences inherent in the various theoretical approaches. In addition, comparison is made of theoretical results for ejection angles larger than 0° to illustrate the degree to which results of these treatments agree for the rest of the spectrum of electrons. Atomic units are used throughout except as otherwise stated.

II. THEORY

The classical trajectory Monte Carlo technique [8, 9] is a simulation of an ion-atom collision in which a large ensemble of initial electronic configurations is sampled in order to reproduce as well as possible the quantum-mechanical position and momentum distributions and therefore the wave function. The subsequent motion of the projectile, target electron (or electrons), and target core is then followed by solving the classical Hamilton equations for a sequence of time steps through the collision. Once the particles have separated, knowledge of their positions and momenta allow determination of the doubly differential ionization cross section.

It is our goal here to examine the ejection of electrons into a very small forward cone about 0° in the laboratory

and for an impact velocity of 7.75 a.u. Consequently, a very large ensemble of trajectories was necessary to provide sufficient counts to resolve the small cross section. To this end, a simulation consisting of 9.1×10^7 trajectories was utilized. This ensured that statistical errors in the doubly differential cross sections were sufficiently small so that even the features with the smallest cross section could be well resolved. For example, the electron-capture-to-the-continuum (ECC) cusp diminishes rapidly with increasing angle for the collision system under consideration here and matching the narrow angular acceptance of the experiment is therefore crucial in comparing the CTMC results with the measurements. In the accompanying figures this statistical error is denoted by the error bars indicating the one standard deviation limit.

Since we seek to treat helium in which two electrons are present, we used the independent electron model, which in this case simply requires that we multiply our single-electron result by a factor of 2. We note that the CTMC model treats fully the interaction of the electron with both the target core $V_t(r_t)$ and the projectile $V_p(r_p) = -Z_p/r_p$, where r_t and r_p are the positions of the electron relative to the target core and projectile, respectively. Thus it implicitly includes "two-center" effects such as the dynamic formation of the ECC cusp [10], the "saddle-point mechanism" [11–13], and the modification of the binary peak's shape and magnitude by both collisional and post-collisional interactions [14, 15]. Since we are particularly interested in describing the shape of the binary peak, we utilize a microcanonical distribution in which the interaction with the residual target core V_t is represented by a model potential [16]. The resulting momentum distribution of helium is in good agreement with the corresponding quantum mechanical one in this case [17].

In addition to this quasiclassical method, we also compute here the first Born approximation (FBA) and continuum-distorted-wave (CDW) approximation and compare with the recent distorted-wave strong potential Born (DSPB) calculations of Brauner and Macek [18]. From a quantum-mechanical point of view, the ionization process constitutes the most troublesome reaction channel occurring in ion-atom collisions. Difficulties start with the description of the final state of an electron that has been removed from the target. In principle, this electron interacts with the time-dependent combined field of the target and projectile. However, no exact manageable solution to this problem exists. Different approximations must be developed which are a good representation of the final state of the electron in various regions of the ejected-electron spectrum.

In these quantal approximations the doubly differential ionization cross section for the ejection of an electron into the solid angle $d\Omega$ with energy E is given by

$$\frac{d^2\sigma}{d\Omega dE} = k_t \frac{1}{4\pi v_p^2} \int_{q_{\min}}^{\infty} q dq \int_0^{2\pi} d\phi_q \mid T_{i,f} \mid^2, \qquad (1)$$

where we have assumed infinite masses of the ions, k_t is the electron momentum relative to the target, v_p is the projectile velocity, and $T_{i,f}$ is the transition matrix between the initial and final states. Further, the momentum transfer is given by $\vec{q} = \vec{K}_i - \vec{K}_f$, where $\vec{K}_i$ and $\vec{K}_f$ are the initial and final projectile momenta with respect to the target, ϕ_q is the azimuthal angle of $\vec{q}$, $q_{\min} = \frac{E+E_i}{v_p}$, and E_i is the target ionization potential.

The Born approximation treats the ejected electron as being in the continuum of the target field, in which case the T matrix is

$$T(\vec{k}_t, \vec{q}) = \langle \phi_f^- \mid V_p \mid \phi_i^+ \rangle = -\frac{4\pi Z_p}{q^2} \int d^3 r_t \psi^{-*}_{t,\vec{k}_t}(\vec{r}_t) e^{i\vec{q}\cdot\vec{r}_t} \varphi_{\alpha_i}(\vec{r}_t) \qquad (2)$$

with

$$\phi_i^+ = e^{i\vec{K}_i \cdot \vec{R}_t} \varphi_{\alpha_i}(\vec{r}_t), \qquad (3)$$

$$\phi_f^- = e^{i\vec{K}_f \cdot \vec{R}_t} \psi^-_{t,\vec{k}_t}(\vec{r}_t), \qquad (4)$$

$$\psi^-_{t,\vec{k}_t}(\vec{r}_t) = \frac{e^{i\vec{k}_t \cdot \vec{r}_t}}{(2\pi)^{\frac{3}{2}}} D_t^-(\vec{k}_t; \vec{r}_t), \qquad (5)$$

where $\psi^-_{t,\vec{k}_t}$ is an incoming continuum state of the target with momentum $\vec{k}_t$, D_t^- is a distortion factor, R_t is the position of the projectile with respect to the center of mass of the target, and φ_{α_i} is the initial bound state of the atom. For an electron-target Coulomb interaction ($V_t = -Z_t/r_t$)

$$D_t^-(\vec{k}_t; \vec{r}_t) = D^-(Z_t, \vec{k}_t; \vec{r}_t) \qquad (6)$$

$$= e^{\frac{\pi\alpha_t}{2}} \Gamma(1 + i\alpha_t) \times {}_1F_1(-i\alpha_t, 1, -i(\vec{k}_t \cdot \vec{r}_t + k_t r_t)), \qquad (7)$$

where $\alpha_t = Z_t/k_t$.

Provided that the impact velocity is high enough or the projectile charge is small enough, the FBA approximation is well suited to describe the bulk of the spectra of ejected electrons with the exception of $\vec{k}_t$ values close to $\vec{v}_p$. In this region, the final interaction of the ionized electron with the outgoing projectile plays an important role and the final state of the electron becomes similar to a continuum state of the projectile $\psi^-_{\vec{k}_p, Z_p}(\vec{r}_p)$. Thus the high velocity spectrum of ejected electrons is sometimes decomposed into electrons in either the continuum of the projectile or the continuum of the target. For smaller impact velocities, or larger projectile charges, the target and the projectile are closer to each other in momentum space and this separation becomes inappropriate. That is, the final state of the electron should be described as a continuum state of the two-center Coulomb field of the target and the projectile. Evidence of effects associated with this problem (the so-called "two-center" effects) have been found experimentally and theoretically [19, 1, 10].

One of the most useful descriptions of the final state of the collision after an ionization event is given by the CDW wave function $\xi_f^- = \phi_f^- D^-(Z_p, \vec{k}_p; \vec{r}_p)$ (Belkić [20] and Crothers and McCann [21]). Concerning the electronic degree of freedom, this wave function has the correct asymptotic behavior in the limit of large internuclear

separations. That is, it behaves as a continuum state of the target (projectile) distorted by an eikonal phase due to the Coulomb field of the projectile (target) for small values of r_t (r_p).

Different models have been proposed which make use of the CDW final wave function. The simplest one consists of approximating the initial state by an undistorted (Born) wave function ϕ_i^+. However, it has been shown that this approach produces results which often overestimate the correct doubly differential cross section by as much as an order of magnitude. More elaborate models also include the distortion of the initial state. It has been pointed out by a number of authors [18, 22] that if the initial state is described by a similar form, i.e., the so-called CDW-CDW [23] approximation, the T matrix is divergent. A numerically intensive approach that avoids this problem has been given by Miraglia and Macek [24] making use of the impulse approximation. A simpler approach that avoids the divergence is the continuum-distorted-wave–eikonal-initial-state (CDW-EIS) approximation, in which the initial state is distorted by an eikonal phase associated with the electron-projectile interaction, that is,

$$\eta_i^+ = \phi_i^+ E^+(Z_p, \vec{v_p}; \vec{r_p}) = \phi_i^+ e^{-i\frac{Z_p}{v_p}\ln(v_p r_p + \vec{v_p}\cdot\vec{r_p})}. \quad (8)$$

The resulting CDW-EIS T matrix is

$$T(\vec{k_t}, \vec{q}) = \langle \xi_f^- \mid V_f^\dagger \mid \eta_i^+ \rangle \quad (9)$$

$$= -(2\pi)^{-\frac{3}{2}} \int d^3 r_p e^{-i\vec{q}\cdot\vec{r_p}} E^+(Z_p, \vec{v_p}; \vec{r_p}) \times \nabla_{\vec{r_p}} D^{-*}(Z_p, \vec{k_p}; \vec{r_p}) \times \int d^3 r_t e^{i\vec{s}\cdot\vec{r_t}} \varphi_{\alpha_i}(\vec{r_t}) \nabla_{\vec{r_t}} D_t^{-*}(\vec{k_t}; \vec{r_t}) \quad (10)$$

with V_f the residual ion potential and $\vec{s} = \vec{q} - \vec{k_t}$.

As with the CTMC method, the independent electron model can be utilized. However, the use of a model potential for the electron-target interaction is extremely computationally intensive, whereas a simple analytic formula exists if instead a Coulomb interaction is used with an effective charge. We note that considerable confusion can arise when the choice made for the charge Z_t in the initial and final wave functions is not specified. In principle, the initial state is properly described by either a single- or multiple-zeta Hartree-Fock wave function (see, e.g., [25]), both of which usually lead to very similar results. The single-zeta wave function takes the form of an initial $1s$ state with an effective charge $Z_t^i = 1.6875$. Some authors alternatively adopt the use of the Bohr formula $Z_t^i = \sqrt{-2E_i}$, with the experimental ionization potential $E_i = 0.903\,55$ a.u., which then yields $Z_t^i = 1.344$. However, if the latter is used, the initial momentum distribution is not properly represented. Similarly, one must choose an effective charge for the final continuum state of the electron and one could use the same charge as used in the initial state. Despite the fact that the initial and final state are not orthogonal, it has become customary to adopt different charges for the initial and final states. This is the case for conventional CDW-EIS calculations [1], which use $Z_t^f = 1.344$. The only common factor in each of these approaches is the value of E_i entering Eq. (1). It is difficult to say which of these choices actually gives the best description.

To circumvent the difficulties in making these choices of effective charges, we have performed the CDW-EIS calculation using the same model potential as we used in the CTMC calculation. This involves making a partial wave expansion for the electronic wave function and computing all the radial integrals numerically. To our knowledge this is the first time such CDW-EIS calculations have been performed. We note that this approach has previously been taken in the FBA [26]. To illustrate the variation of the CDW-EIS result for these choices, we plot in Fig. 1 calculations using the same initial state ($Z_t^i = 1.6875$) and choices for Z_t^f, the final effective charge, of 1.0, 1.344, and 2.0, along with that found using the model potential. Depending on which feature of the spectrum one wishes to describe, one choice or another seems to agree best with the model potential result. For extremely low electron energies or in the binary peak region, the conventional choice of effective charges agrees reasonably well with the model potential results. However, for intermediate energies (here $20 \leq E_e \leq 1000$ eV), those around the cusp, a final effective charge of 2.0 agrees best.

In the spirit of the CDW-EIS model, considering the electron as being in the field of the projectile and residual target ion, one might assume that an asymptotic target charge of 1.0 would yield the correct behavior of the cross section. However, it is seen from this comparison that this is not the case. This is not difficult to understand since what determines the magnitude of the T matrix is

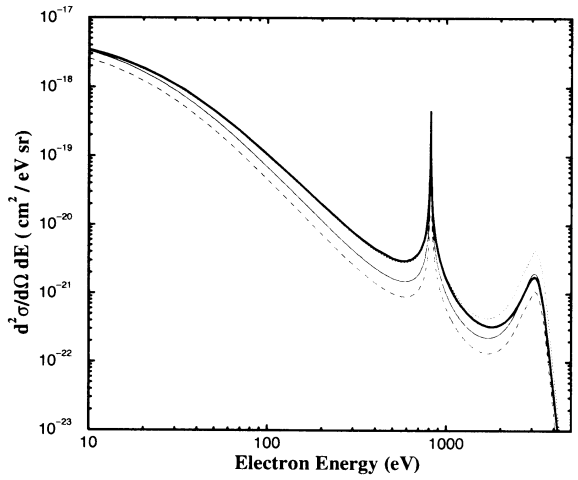

FIG. 1. Comparison of the CDW-EIS doubly differential ionization cross section for 1.5-MeV/u F^{9+} colliding with helium when various common choices are made for the final effective charge Z_t^f. The solid line indicates the conventional choice 1.344, the dashed line indicates the result with $Z_t^f = 1.0$, and the dotted line indicates the result with $Z_t^f = 2.0$. In addition, the heavy solid line is the result found from the present model potential CDW-EIS treatment. All curves are for 0° electron ejection in the laboratory frame.

the behavior of the continuum radial wave function near the origin (collision regime) rather than in the aysmptotic region. Since electron capture occurs primarily at very small impact parameters, the ECC electrons are produced at very small distances where the model potential tends to the same value as a Coulomb potential with an effective charge of 2.0.

In the following section we will display theoretical calculations utilizing the FBA and CDW-EIS results with effective charges ($Z_t^i = 1.6875$ and $Z_t^f = 1.344$) and the CDW-EIS approximation using a model potential. In addition, we include for comparision the DSPB approximation results of Brauner and Macek [18].

The point of view taken in the strong potential Born approximation [27,28] is to employ an expansion in powers of the smaller charge of the target rather than of the projectile when a highly charged ion impinges upon an atom of low atomic number. Thus the DSPB theory expands in terms of a smaller quantity and seeks to thereby improve convergence of the perturbative expansion. The strong potential $V_p = -Z_p/r_p$ is retained to all orders in the Green's function G_p in this approximation where $Z_p \gg Z_t$ and thus the name "strong potential Born." The DSPB calculations were performed using the so-called Bates-Griffing independent electron model, which uses an effective charge of $Z_t^i = Z_t^f = 1.345$.

III. RESULTS

Comparison is made in Fig. 2 of the results of all these theoretical approaches with the measurements of Lee *et al.* [7] of the doubly differential ionization cross section at 0° in the laboratory frame. The angular acceptance of the apparatus was approximately ±(0.6°–0.65°) [29].

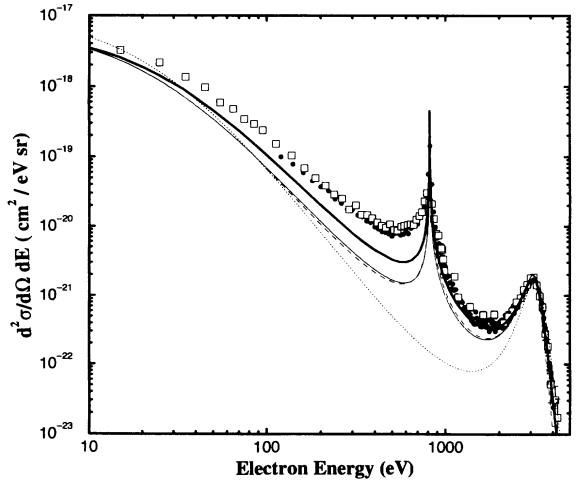

FIG. 2. The spectrum of electrons ejected at 0° in the laboratory for collisions of 1.5-MeV/u F^{9+} with helium. The solid circles indicate the experimental data of Lee *et al.* [7], the open squares the present CTMC result, the solid line the conventional effective charge CDW-EIS result, the heavy solid line the model potential CDW-EIS result, the dotted line the FBA, and the dashed line the DSPB calculation of Brauner and Macek [18].

Thus the CTMC results used as close a narrow acceptance as was possible consistent with having a reasonably small associated statistical error. In particular, we used an angular acceptance of ±1°. Using a reasonable value for this acceptance is important because the doubly differential cross section within about 50 eV on either side of the ECC cusp changes rapidly with increasing ejection angle for this highly charged ion impact and for this high impact velocity. The perturbation theory results were all computed at 0° without any convolution over ejection angles. Such a convolution would only change the curves displayed very near (e.g., within 20 eV) the cusp.

As the figure indicates, the agreement between the measurements and the CTMC simulation is excellent. For the lowest electron energies, the measurements appear to fall off, diverging from the calculation, but this effect has been ascribed by Lee *et al.* [7] to the behavior of their spectrometer. Since the FBA treats the ejected electron as evolving only in the field of the target, the ECC cusp is not present it this case. The CDW-EIS and DSPB approaches, however, do display the cusp, but do not reproduce the correct degree of asymmetry of the peak. The model potential CDW-EIS shows an appreciable improvement over the effective charge models.

Figure 3 displays enlarged views of both the cusp and binary peak regions of the spectrum. Regarding the cusp, this figure shows that the effective charge CDW-EIS and DSPB results are remarkably similar even though they come from rather different theoretical approaches. Both theories yield a shape which is much more symmetric about the cusp center than does CTMC or the experiment. The origin of this behavior lies in the relationship between the degree of symmetry and the distribution of angular momenta of the electron which in the final state ends up in the low-lying continuum of the projectile. In fact, viewing the cusp in the limit of large principal quantum numbers as composed of electrons lying in Rydberg

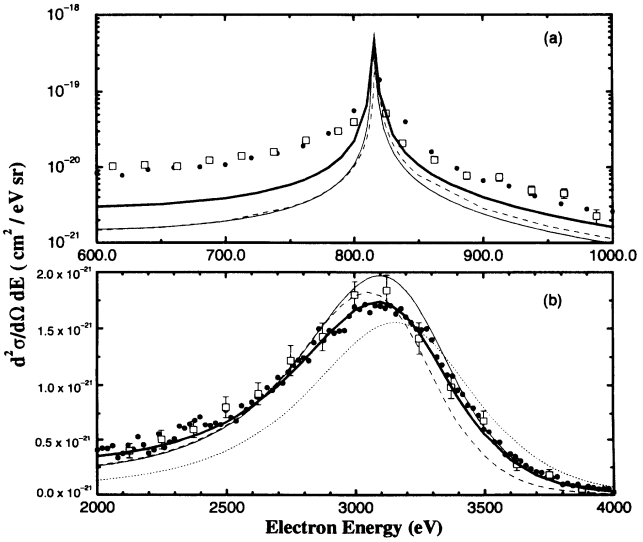

FIG. 3. In (a) and (b) we display enlarged views of the ECC and binary peak regions of the 0° spectrum, respectively. The symbols are as indicated in the caption to Fig. 2.

states [30] the asymmetry parameter $\beta_1(n)$ (cusp multipole) is related to the expectation of the projection of the dipole operator d_z by the relation

$$\langle d_z \rangle = -\frac{n}{2Z_p}(n^2-1)^{\frac{1}{2}}\beta_1(n). \tag{11}$$

Thus the good match CTMC makes of the asymmetry of the cusp is a strong indication of its good representation of the orientation present in the ECC electrons. Recent work has sought to show the reasonable agreement with experiment of the CTMC coherence parameters for lower-lying states of hydrogen in charge transfer collisions (H^+ + He) at intermediate energies, where measurements exist [31]. Certainly, high-order terms in the perturbation series expansion contribute to this behavior.

Also indicated by Fig. 3 is the good agreement between CTMC and the measurements of the binary peak. The experimental points lie within all the CTMC error bars on this linear plot, with the largest disagreement coming just at the top of the peak. In contrast, the effective charge perturbation theory results do not fit the shape nearly as well. The CDW-EIS peak is centered better on the experimental one than the DSPB result, probably because of the choice of initial target effective charge, since the binary peak reflects essentially the initial electronic momentum distribution. The model potential CDW-EIS gives excellent agreement with the measurements in the binary peak region.

In addition, as one can see by reference to the FBA result [32], the two-center theories, as well as the experiment, show that the binary peak is shifted to lower energy. At least for 0° ejection, this shift seems to be due to the fact the binary electron, which attains a velocity twice that of the projectile, is post-collisionally retarded by the strong residual interaction with both the target and projectile which are behind it. Whether this simple idea is valid for larger ejection angles is subject to debate, and a number of works have sought to explore the shift of the peak position for a variety of bare and clothed ions [15]. The shift may also be interpreted as arising simply from the fact that the cross section for two-center electrons (i.e., those on the high-energy side of the cusp), which is sloping downward as electron energy increases, is added to the contribution from the binary electrons which themselves form a peak, reflecting the initial momentum distribution. The result of adding this decreasing function on the low-energy side to the peak is to shift its maximum to the left.

It is also interesting to display the behavior of the doubly differential ionization cross section for angles larger than 0°, to allow a further comparison between the quantal perturbation theories and the CTMC model, to give a general impression of the behavior of the ejected electron spectrum, and perhaps to motivate further experiment for this and other similar collision systems. To this end, we display in Figs. 4 and 5 the results of the FBA, CDW-EIS, and CTMC treatments for ejection to 10°, 30°, 50°, 90°, 120°, and 150°. Absent in these spectra is the ECC cusp, which diminishes rapidly with increasing angle, as we have noted above. Only a small remnant is seen at 10° and by 30° it is completely missing. The

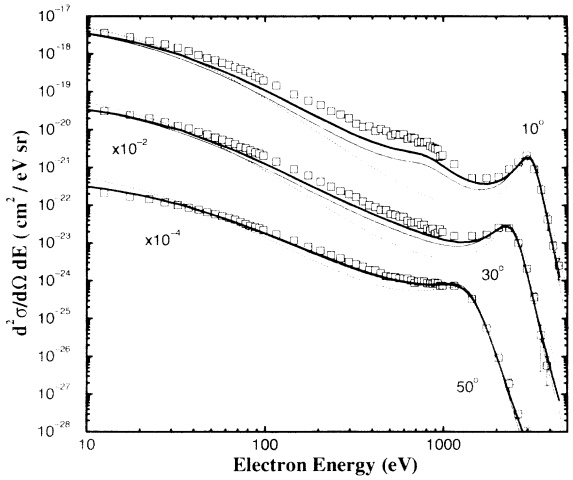

FIG. 4. The CTMC, CDW-EIS, and FBA results are compared for electron ejection at 10°, 30°, and 50°, respectively. The symbols are as indicated in the caption to Fig. 2. The 30° and 50° results have been divided by factors of 10^2 and 10^4, respectively.

binary peak is seen to shift to lower energies, roughly in accord with the binary encounter model, which predicts that the binary peak energy $E_b = 2v_p^2\cos^2\theta - E_i$, where θ is the electron ejection angle, the other quantities having been previously defined. As we have noted, the peak is shifted further to lower energies than given by this formula. Eventually, the binary peak shifts to sufficiently low energies that it ceases to be a separately resolvable feature of the spectrum.

Even at 10°, the importance of the two-center effects leading to the cusp formation is evident in that the FBA is still much too small in the region where the projectile and electron velocities are nearly the same. By 50°, where the projectile and electron trajectories diverge to

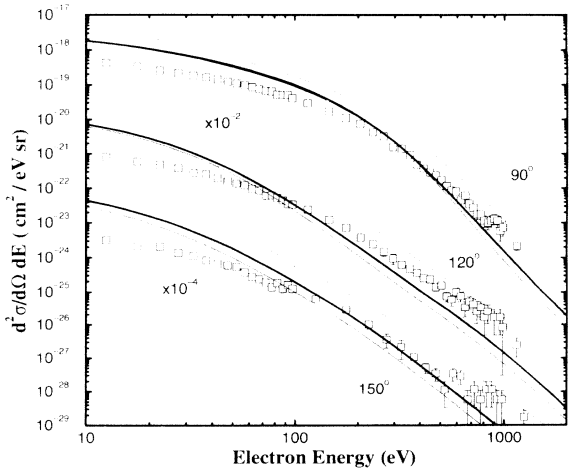

FIG. 5. The CTMC, CDW-EIS, and FBA results are compared for electron ejection at 90°, 120°, and 150°, respectively. The symbols are as indicated in the caption to Fig. 2. The 120° and 150° results have been divided by factors of 10^2 and 10^4, respectively.

a much greater extent, the FBA agrees much better with the two-center treatments. Also, as the angle is increased from 10° to 50°, CTMC and CDW-EIS come into better agreement. The shift to lower energies of the binary peak in these results compared to the FBA is clear as well. For much larger angles, the CTMC results begin to be much lower than the perturbation theory curves for low electron energies. This behavior has been seen for a long time in comparison of CTMC results with experiment for the singly differential cross section at large angles and has been discussed in detail for the doubly differential cross section in ionizing $H^+ + H$ collisions [33] and from a theoretical point of view which considers the classical limit of ionization in fast ion-atom collisions [34].

In brief, these studies have shown that in the case of small momentum transfers, such as the large-impact parameter collisions which result in backward scattering of slow electrons, the classical behavior differs significantly from the correct quantum result. However, for larger momentum transfers, a much better behaved classical limit exists and the forward and high electron energy portions of the spectrum are thus good approximations to a more complete quantum-mechanical treatment. Thus, at backward angles and small energies, the perturbation theory results should be considered more reliable. For larger ejection energies in this angular regime, the CTMC results lie in between the CDW-EIS and FBA results. As mentioned previously [33], for small ejection angles the CTMC results seem to be the best, but as the ejection proceeds to angles larger than 90°, for example, a smooth curve which follows the CDW-EIS solution at low energies and the CTMC result at high energies seems to be the best prediction of the actual ejected electron spectrum.

IV. SUMMARY

We have computed the first Born and continuum-distorted-wave–eikonal-initial-state approximations for the ejected electron spectrum in collisions of 1.5-MeV/u F^{9+} with helium at 0°, 10°, 30°, 50°, 90°, 120°, and 150° in the laboratory frame. In addition, we have performed a very large classical trajectory Monte Carlo simulation of the collision consisting of almost 100 million trajectories. We find the agreement between the experimental measurements at 0° of Lee *et al.* [7] and the CTMC results, including the ECC cusp asymmetry, to be excellent, better than the agreement with the quantal perturbation theories. However, inclusion of a model potential to represent the electron-target interaction appreciably improves the CDW-EIS result, especially in the binary peak region. We also find very little difference between the effective charge CDW-EIS result and the distorted-wave strong potential Born approximation of Brauner and Macek [18], except near the binary peak. This difference we attribute to the difference in choice of initial target effective charge and thus initial momentum distribution. Finally, for angles larger than 0° we have contrasted the behavior of the CTMC, CDW-EIS, and FBA results, indicating the energy and angle regimes in which each is most likely to be reliable, as a guide to further experiment and to provide a general description of the full ejected-electron spectrum.

ACKNOWLEDGMENTS

This research was sponsored by the U.S. Department of Energy under Contract No. DE-AC05-84OR21400 managed by Martin Marietta Energy Systems Inc. We wish to thank Michael Brauner for the data files we used to plot the DSPB results and Joe Macek and Joachim Burgdörfer for helpful discussions. Additional support is also acknowledged by C.O.R. from the National Science Foundation. In addition, we wish to thank David Dean for help in parallelizing the CTMC codes for use on the ORNL Intel i860 multicomputer, which was used to generate about half of the trajectories used in the present simulation.

[1] P.D. Fainstein, V.H. Ponce, and R.D. Rivarola, J. Phys. B **24**, 3091 (1991).
[2] M.E. Rudd, Y.-K. Kim, D.H. Madison, and T.J. Gay, Rev. Mod. Phys. **64**, 441 (1992).
[3] See, for example, P.V. Dressendorfer, Nucl. Instrum. Methods Phys. Res. Sect. B **40/41**, 1291 (1989); W.E. Price and J.R. Cross, *ibid.* **40/41**, 1306 (1989).
[4] G. Kraft, Nucl. Sci. Appl. **3**, 1 (1987).
[5] For example, R. Katz, in *Quantitative Mathematical Models in Radiation Biology*, edited by J. Kiefer (Springer, Berlin, 1988), p. 57.
[6] L.H. Toburen, N.F. Metting, and L.A. Brady, Nucl. Instrum. Methods Phys. Res. Sect. B **40/41**, 1275 (1989).
[7] D.H. Lee, P. Richard, T.J.M. Zouros, J.M. Sanders, J.L. Shinpaugh, and H. Hidmi, Phys. Rev. A **41**, 4816 (1990).
[8] R. Abrines and I.C. Percival, Proc. Phys. Soc. **88**, 81 (1966).
[9] R.E. Olson and A. Salop, Phys. Rev. A **16**, 531 (1977).
[10] C.O. Reinhold and R.E. Olson, Phys. Rev. A **39**, 3861 (1989).
[11] R.E. Olson, Phys. Rev. A **27**, 1871 (1983).
[12] R.E. Olson, Phys. Rev. A **33**, 4397 (1986).
[13] R.E. Olson, T.J. Gay, H.G. Berry, E.B. Hale, and V.D. Irby, Phys. Rev. Lett. **59**, 36 (1987).
[14] O. Jagutzki, S. Hagmann, H. Schmidt-Böcking, R.E. Olson, D.R. Schultz, R. Dörner, R. Koch, A. Skutlartz, A. González, T.B. Quinteros, C. Kelbch, and P. Richard, J. Phys. B **24**, 2579 (1991).
[15] W. Wolff, H.E. Wolf, J.L. Shinpaugh, J. Wang, R.E. Olson, P.D. Fainstein, S. Lencinas, U. Bechthold, R. Herrmann, and H. Schmidt-Böcking, J. Phys. B **26**, 4169 (1993).
[16] R.H. Garvey, C.J. Jackman, and A.E.S. Green, Phys. Rev. A **12**, 1144 (1975).

[17] C.O. Reinhold and C.A. Falcón, Phys. Rev. **33**, 3859 (1986).
[18] M. Brauner and J.H. Macek, Phys. Rev. A **46**, 2519 (1992).
[19] N. Stolterfoht, D. Schneider, J. Tanis, H. Altervogt, A. Salin, P.D. Fainstein, R. Rivarola, J.P. Grandin, J.N. Scheurer, S. Andriamonje, D. Bertault, and J.F. Chemin, Europhys. Lett. **4**, 899 (1987).
[20] Dž. Belkić, J. Phys. B **11**, 3529 (1978).
[21] D.S.F. Crothers and J.F. McCann, J. Phys. B **16**, 3229 (1983).
[22] C.O. Reinhold and J.E. Miraglia, J. Phys. B **20**, 1069 (1987).
[23] We have also computed the CDW-CDW approximation and found, as has been known for some time, that the amplitude contains a divergence. For energies below that of the cusp, the singularity is extremely narrow and by neglecting it, much better agreement with the experimental results can be obtained. This is not to say that the singularity is integrable, but rather only to give the impression that the more complete treatment of the intial state seems important to the perturbation treatment for the lower electron energies.
[24] J.E. Miraglia and J.H. Macek, Phys. Rev. A **43**, 5919 (1991).
[25] E. Clementi and C. Roetti, At. Data Nucl. Data Tables **14**, 177 (1974).
[26] D.H. Madison, Phys. Rev. A **8**, 2449 (1973); S.T. Manson, L.H. Toburen, D.H. Madison, and N. Stolterfoht, *ibid.* **12**, 60 (1975).
[27] See J.H. Macek, J. Phys. B **24**, 5121 (1991), and references therein.
[28] K. Taulbjerg, R.O. Barrachina, and J.H. Macek, Phys. Rev. A **41**, 207 (1990).
[29] D.H. Lee, Ph.D. thesis, Kansas State University, 1990.
[30] See, for example, J. Burgdörfer, Phys. Rev. A **33**, 1578 (1986).
[31] C.J. Lundy, R.E. Olson, D.R. Schultz, and J.P. Pascale, J. Phys. B **27**, 935 (1994).
[32] We have also computed the binary encounter approximation [T.F.M. Bonsen and L. Vriens, Physica (Utrecht) **47**, 307 (1970)], a theory describing the binary encounter of the electron with the projectile as a convolution of the initial electronic momentum distribution with the elastic scattering in the field of the projectile, a one-center approximation. We find that it agrees here closely with the FBA.
[33] D.R. Schultz, R.E. Olson, C.O. Reinhold, M.W. Gealy, G.W. Kerby, Y.-Y. Hsu, and M.E. Rudd, J. Phys. B **24**, L599 (1991).
[34] C.O. Reinhold and J. Burgdörfer, J. Phys. B **26**, 3101 (1993).